Contents lists available at ScienceDirect

Clinical Immunology

journal homepage: www.elsevier.com/locate/yclim





Integration of multi-omics analysis reveals metabolic alterations of B lymphocytes in systemic lupus erythematosus

Cristian Iperi ^a, Álvaro Fernández-Ochoa ^b, Jacques-Olivier Pers ^a, Guillermo Barturen ^{c,d}, Marta Alarcón-Riquelme ^{c,e}, PRECISESADS Flow Cytometry Study Group, PRECISESADS Clinical Consortium, Rosa Quirantes-Piné ^f, Isabel Borrás-Linares ^b, Antonio Segura-Carretero ^b, Divi Cornec ^a, Anne Bordron ^{a,1}, Christophe Jamin ^{a,*,1}

- a LBAI, UMR1227, Univ Brest, Inserm, Brest, France
- ^b Department of Analytical Chemistry, University of Granada, Granada, Spain
- ^c GENYO, Centre for Genomics and Oncological Research Pfizer, University of Granada, Andalusian Regional Government, PTS Granada, Granada, Spain
- ^d Department of Genetics, Faculty of Sciences, University of Granada, Granada, Spain
- ^e Institute for Environmental Medicine, Karolinska Institutet, Stockholm, Sweden
- f Research and Development of Functional Food Centre (CIDAF), Health Science Technological Park, Granada, Spain

ARTICLE INFO

Keywords: Systemic lupus erythematosus Multi-omics B lymphocytes Metabolomics MOFA

ABSTRACT

Objective: To link changes in the B-cell transcriptome from systemic lupus erythematosus (SLE) patients with those in their macroenvironment, including cellular and fluidic components.

Methods: Analysis was performed on 363 patients and 508 controls, encompassing transcriptomics, metabolomics, and clinical data. B-cell and whole-blood transcriptomes were analysed using DESeq and GSEA. Plasma and urine metabolomics peak changes were quantified and annotated using Ceu Mass Mediator database. Common sources of variation were identified using MOFA integration analysis.

Results: Cellular macroenvironment was enriched in cytokines, stress responses, lipidic synthesis/mobility pathways and nucleotide degradation. B cells shared these pathways, except nucleotide degradation diverted to nucleotide salvage pathway, and distinct glycosylation, LPA receptors and Schlafen proteins.

Conclusions: B cells showed metabolic changes shared with their macroenvironment and unique changes directly or indirectly induced by IFN- α signalling. This study underscores the importance of understanding the interplay between B cells and their macroenvironment in SLE pathology.

1. Introduction

B cells are immune cells specialised in the production and secretion of antibodies against pathogens and cancer cells. In systemic lupus erythematosus (SLE), after the loss of tolerance, B cells become autoreactive and develop antibodies that target and destroy cells and tissues. This causes a periodic inflammatory reaction and tissue necrosis in specific areas, denoting an active disease status known as "flare" [1]. The peculiar autoantibodies primarily target nuclear structures as well as antigens related to other structures and functions [2]. B cells also contribute to the SLE disease through cell-to-cell contact, production of inflammatory cytokines [3], and due to defective IL-10-producing B cells unable to dampen inflammation [4]. Thus, interferon (IFN)- α expression

is correlated with SLE severity and is used to classify patients [5]. The majority of the studies to detect novel disease markers and treatments for SLE focussed on single omics approaches in combination with clinical data. A step further was made with the IMI PRECISESADS project aiming to characterize autoimmune diseases based on a multi-omics approach, providing a wide vision of the disease changes in transcriptomics, metabolomics and clinics [6,7]. The present work investigated the changes occurring in the blood macroenvironment of patients with SLE from PRECISESADS and examined how these changes affect the transcriptome of B cells. Moreover, blood metabolites such as nutrients and signalling molecules shape the natural macroenvironment in which mature B cells perform their physiological functions [5,8]. Plasma and urine contain the metabolites circulating in the bloodstream and the

^{*} Corresponding author at: LBAI, UMR1227, Laboratory of Immunology, CHU Morvan, BP824, F29609 Brest, France. *E-mail address*: christophe.jamin@univ-brest.fr (C. Jamin).

¹ These two last authors contributed equally to this work.

Table 1Number of samples available in the study.

Samples	B-cell transcriptome	Whole-blood transcriptome	Plasma metabolome	Urine metabolome
CTRL	27	508	55	55
SLE	36	363	46	46
CTRL integrated with MOFA	22	46	55	55
SLE integrated with MOFA	11	35	46	46

Number of systemic lupus erythematosus (SLE) and control (CTRL) samples from the PRECISESADS cohorts are indicated. Number of samples shared between the transcriptomic and metabolomic analyses in the MOFA integration analysis are also indicated.

metabolites actively removed from it, respectively. They were therefore used to analyse the blood macroenvironment. Another approach includes whole-blood transcriptome analysis, which approximates the global gene expression changes among the immune cell types. The overlap between the transcriptome and metabolome defines the blood macroenvironment. Changes in the B-cell transcriptome were linked to the macroenvironmental changes, and validated by comparing the results with a previously published database used as a validation dataset matching for study design, technology and samples, including the B-cell transcriptome from SLE patients and healthy controls (CTRL) [9]. Differences in B cells in IFN-α-positive and IFN-α-negative SLE subgroups were investigated, approving the results by comparison with the validation dataset and by machine learning approaches. Finally, the metabolomics and transcriptomics analyses were integrated to identify not only the common Multi Omics Factor analysis (MOFA) factors distinguishing patients with SLE from CTRLs but also the genes and mass spectrometry peaks primarily contributing to them. Overall, their contributions together with the clinical data have led to innovations in elucidating the underlying biological processes involved in SLE.

2. Material and methods

2.1. Samples and cohort selection

The cross-sectional dataset from the European PRECISESADS cohort (number NCT02890121 in ClinicalTrials.gov) aimed to reclassify the autoimmune diseases by the molecular signature including clinical (Table S1) and multi-omics information. The patient selection and quality control have previously been described in detail [6,7]. PRECISESADS adhered to the standards set by International Conference on Harmonization and Good Clinical Practice (ICH- GCP), and to the ethical

was partitioned for supplementary analysis. Purified B lymphocytes were isolated from a fraction of the second aliquot (36 SLE and 27 CTRL; Table 1 and Fig. S1). Moreover, 101 paired samples of plasma and urine were collected (46 SLE and 55 CTRL).

2.2. Transcriptome data generation

The whole blood and sorted B cell samples were sequenced using a Novaseq 5000 and a NextSeq 500, respectively, with an average coverage per sample of 13.6 Million reads for the former and 29.3 Million reads for the latter. The FastQ files were aligned to the UCSC Homo sapiens reference genome (hg19) and annotated to GENCODE 19 with STAR v2.5.2 [11] using two-pass mapping strategy with default parameters. Gene quantification was performed using RSEM v1.2.31 [12]. At the end, 363 SLE and 508 CTRL whole-blood transcriptomes and 36 SLE and 27 CTRL B-cell transcriptomes were profiled (Table 1). A validation dataset was downloaded from the GEO database (GSE149050). It contains the B-cell transcriptomes from 24 CTRLs and 64 patients with SLE, including 30 IFN- α -positive and 34 IFN- α -negative patients. The validation dataset patients and PRECISESADS dataset patients were matched for treatments and percentage of patients taking treatments.

2.3. Analysis of B-cell purity

B-cells were sorted by CD19 positive selection (Miltenyi) and the purity checked by flow cytometry. After extraction, the B-cell RNA purity of SLE and CTRL samples was evaluated using two tools based on immune cell-specific gene signatures, Macroenvironment Cell Populations-counter [13] on R with default parameters and CIBER-SORTx [14] (leukocyte panel LM22; online version, https://cibersortx.st anford.edu/). Samples with digital purity lower than 90% were excluded from the subsequent analysis. The final number of samples included 29 SLE and 22 CTRL samples (Table 2).

2.4. IFN- α classification in whole-blood and B-cell samples

Patients with SLE were classified into IFN- α -positive and IFN- α -negative subgroups using an IFN- α score established based on the Kirou score [15] approach. This approach measures the IFN- α response using the transcriptome of 20 genes [7] (SIGLEC1, IFIT3, IFI6, LY6E, MX1, USP18, OAS3, IFI44L, OAS2, IFIT1, EPST11, ISG15, RSAD2, HERC5, OAS1, IFI44, SPATS2L, PLSCR1, IFI27, and RTP4) in addition to six IFN- α -associated genes (EIF2AK2, GBP1, IRF1, SERPING1, CXCL10, FCGR1A). Gene expression levels were quantified in terms of raw reads normalised to the total number per sample, and the score was calculated as the expression of each gene (g) for each SLE sample (s) with the mean expression divided by the standard deviation of the CTRLs as follows:

 $\label{eq:Zinterferonactivityscore} Zinterferonactivityscore = \frac{gene expression_{gs} - mean(gene expressionCTRL population)}{standard deviation(gene expressionCTRL population)}$

principles written in the Declaration of Helsinki (2013). Each patient signed an informed consent prior to study inclusion. The Ethical Review Boards of the 19 participating institutions approved the protocol of the cross-sectional study. This study was a pre-planned substudy to be specifically conducted in the SLE population, defined by the American College of Rheumatology of 1997 criteria [10] and fulfilling the CONSORT statements (Supplementary data). In brief, whole blood samples from the SLE (n=363) and CTRL (n=508) groups were divided into two aliquots: the first contained all immune cell types, and the second

The higher the Z interferon activity score (Z-score) for a particular gene compared to the CTRLs, the higher the IFN- α activation of that gene. By means of the Z-score, samples were grouped using the hierarchical clustering of the Complexheatmap package v2.12.0 [16] on R. This showed two subgroups of 22 IFN- α -positive and 7 IFN- α -negative purified B-cell samples (Fig. 1A). Two CTRLs showed a high IFN score in B cells and were excluded from further analyses (Table 2). Similarly, SLE whole-blood samples were classified into 269 IFN- α -positive and 94 IFN- α -negative samples.

 Table 2

 B-cell samples from systemic lupus erythematosus and controls of the PRECISESADS cohorts were discarded from further analysis based on the criteria used to extract those filtered.

Individuals	Unfiltered samples	B cells with digital purity $<$ 90% in MCP	B cell < 90% purity/high specific cell type contamination in Cibersort	IFN-α-positive CTRL samples	Total filtered samples
CTRL total SLE IFN-α-positive	27 samples 36 samples 25 samples	3 samples 6 samples 2 samples	1 sample 1 sample	2 samples	22 samples 29 samples 22 samples
SLE IFN-α-negative SLE	11 samples	4 samples			7 samples

CTRL: controls; MCP: Microenvironment Cell Populations; SLE: systemic lupus erythematosus.

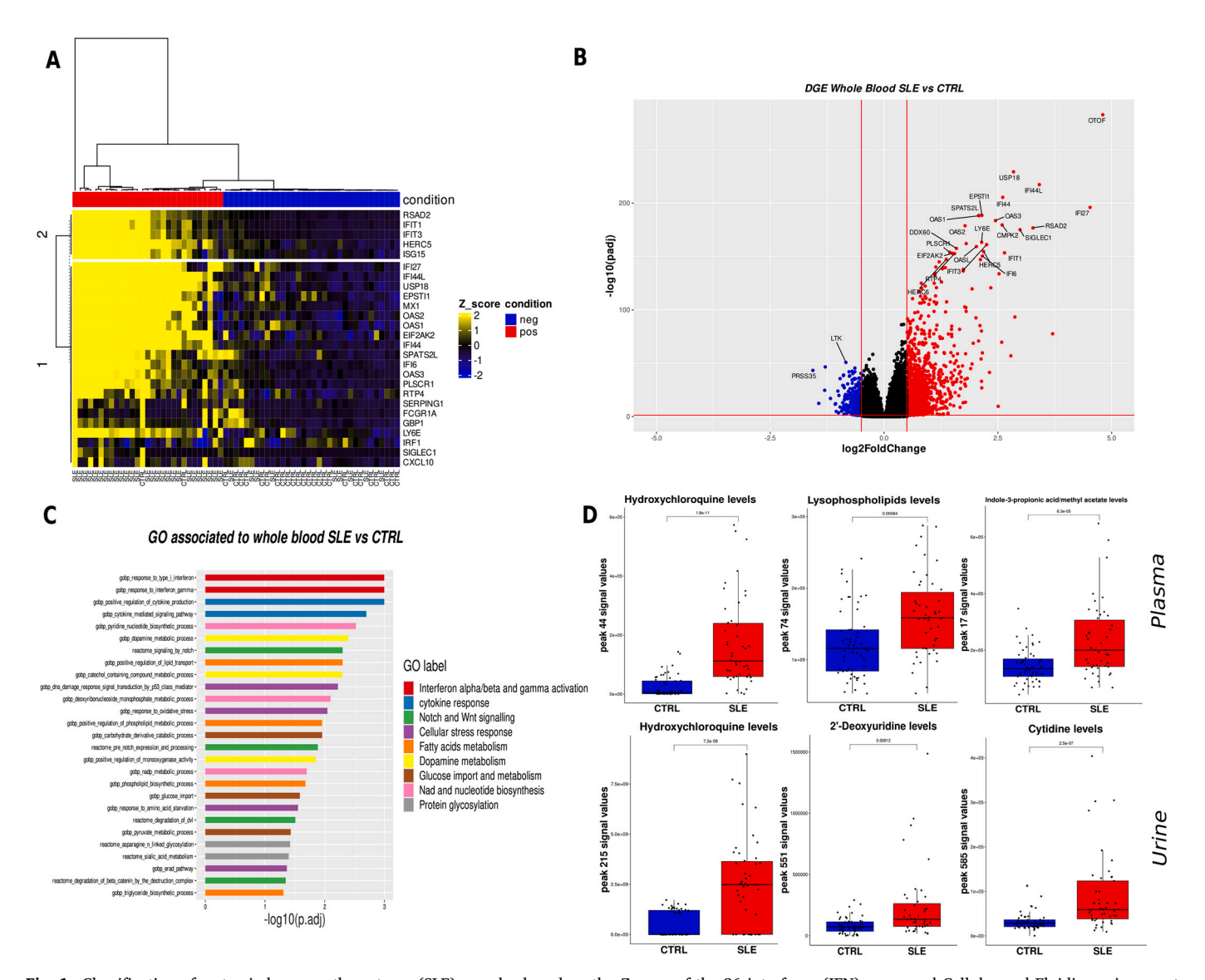


Fig. 1. Classification of systemic lupus erythematosus (SLE) samples based on the *Z*-score of the 26 interferon (IFN) genes and Cellular and Fluidic environment changes. A) SLE and control (CTRL) unfiltered samples are indicated at the bottom of the heatmap. The classification into positive and negative samples was obtained by hierarchical clustering based on the *Z*-score of the 26 IFN-α genes measured for each gene within each sample. A single square corresponds to the *Z*-score of a specific IFN-α gene for an individual sample. Euclidean distance and Ward's method have been used for hierarchical clustering. B) Volcano plot of the differential gene expression (DGE) analysis of the CTRL samples vs patients with SLE in the PRECISESADS whole blood dataset. Downregulated and upregulated genes are depicted in blue and red, respectively. Only the top 15 genes in each category are indicated. The significance thresholds, shown as red lines, are |Log2FC| > 0.5 and false discovery rate (FDR) < 0.05C) Gene set enrichment analysis (GSEA) of the whole-blood transcriptome using the gene ontology (GO) and Reactome libraries. The categories of metabolic pathways and their adjusted *p*-values for each GO pathway are depicted. D) Levels of metabolites in plasma and urine of CTRL and SLE samples are depicted in blue and red, respectively. Significance was calculated using the Mann-Whitney test. (For interpretation of the references to colour in this figure legend, the reader is referred to the web version of this article.)

2.5. Differential gene expression analysis

All differential gene expression (DGE) analyses provided raw gene counts as input for DESeq2 [17], used with default parameters. Sex and age were included in the model as confounding factors. Although present in all subgroups, the treatments were not included because of their heterogeneity and variable co-administration with other drugs and medications. The threshold values to identify the DEGs were set to | Log2FC| >0.5 and false discovery rate (FDR) <0.05. Nominal p-values were adjusted for multiple testing using the FDR method.

2.6. Gene set enrichment analysis

The gene set enrichment analysis was performed using GSEA [18] v4.1.0 for the Linux system. The matrix counts were uploaded directly into GSEA, and the libraries explored included Reactome v.2022.1 and Biological Processes (BP) v.2022.1. The EnrichR [19] tool v2022 was also used, uploading the genes identified as upregulated and down-regulated in the DGE analysis separately. For both, only processes with a Benjamini–Hochberg adjusted p-value <0.05 were considered.

2.7. Metabolomics data generation and statistical analysis

Metabolomics data were pre-processed according to the protocol described in previous PRECISESADS study [7]. In total, 531 and 1022 peak intensities were identified in plasma and urine samples, respectively, and compared between the SLE and CTRL groups. The log2FC value was calculated as the log2 of the ratio between the median peak signals in SLE and in CTRL for each peak. The p-value was estimated using the non-parametric Mann-Whitney test and corrected using the FDR method. Metabolites with a statistically significant difference (FDR < 0.05) were used for further analysis. When comparing groups divided according to sex and age (younger than 35 – between 35 and 50 – and older than 50), all peaks were not significantly different, excluding a significant contribution of these confounding factors. Although present in all subgroups, the treatments were not tested because of their heterogeneity and variable co-administration with other medications.

2.8. Metabolomics peak annotation

The plasma and urine peaks were annotated using the Ceu Mass Mediator tool [20] in the CMMR R package [21]. The data used included the mass-to-charge (m/z) ratio and retention time (rt). The metabolites were filtered by those identified or predicted according to the Human Metabolome Database (HMDB) [22]. The MS/MS data, when available, were analysed using GNPS [23], and the results matched with those obtained with only m/z and rt.

2.9. Machine learning validation

The extreme gradient boosting model (XGBoost) based on the random forest machine learning method was performed on CTRL and IFN- α -positive SLE B cells from the PRECISESADS and the validation datasets, training the model with seven-eighths of the samples and testing with the remaining. The xgboost package on R was used setting as parameters max_depth = 3, eta = 0.1, gamma = 0, min_child_weight = 1. The genes in the model came from the GSEA gene sets.

2.10. Multi-omics factor analysis

MOFA+ is an integration method catching the common variability among the datasets provided as input. MOFA calculates factors made up of a linear combination of the multi-omics variables and selects the most relevant contributors after discarding the not relevant ones by regularization. It provides a few easily interpretable factors due to the limited number of contributors to explore, compared to other dimension

reduction methods as principal component analysis. Its application in public datasets can dig deeper into the data compared to conventional statistical analysis in any field. The only requirement is to have multiomics data from the same samples or patients. MOFA [24] was used according to the developer's instructions (https://biofam.github. io/MOFA2/), where further details about the algorithm are available. The transcriptome data from B cells and whole blood were transformed using the Variance Stabilising Transformation (VST) function in R to make the data approximately homoscedastic. To shrink the size of the matrices data, the top 5000 genes were selected, based on the highest variance obtained from the size factor normalised data. The plasma and urine metabolomics data were log-transformed to improve their Gaussian distribution. All peaks were included in the analysis. The number of samples used for MOFA is reported in Table 1. The number of MOFA factors was determined after the evaluation of the results, from 3 to a maximum of 30, to avoid factor redundancy, as explained in the MOFA+ [24] instructions. The Factors 18 and 20 included at least three MOFA factors (Factor 2, 4, 5 and 9) with significant separation of SLE from CTRLs (Table S2). Factor 18, which showed the best separation (FDR-corrected Mann-Whitney test), was used for further analysis. In the MOFA factor exploration, only the top 5% genes/peaks with a higher contribution and a contribution weight > 0.50 were studied (Fig. S2). MOFA ran with default parameters and fast convergence. The factors were not correlated with each other, ensuring that the variability cached by the factors came from non-overlapping variations in genes or peaks.

2.11. Clinical data analysis

The 50 clinical features and 49 autoantibody measurements from the PRECISESADS dataset were analysed and correlated with significant Factors 2, 4, 5, and 9 of the MOFA analysis using Pearson correlation. The 157 binary clinical data points were analysed using the Wilcoxon test after dividing the groups into two categories. The nominal p-values were corrected using the Benjamini-Hochberg method.

3. Results

3.1. Exploration of the disease macroenvironment using transcriptomics and metabolomics

The disease macroenvironment of SLE can be subdivided into a cellular macroenvironment—which includes the whole-blood transcriptome—and a fluidic macroenvironment— which includes the plasma and urine metabolome. Compared with CTRL, the DGE analysis of the whole-blood transcriptomic data highlighted 1232 upregulated and 359 downregulated genes. As expected, the top DEGs were components of the IFN response pathway (Fig. 1B). Moreover, GSEA identified increased IFN- α , β , and γ activation and cytokine responses in the patients with SLE (Fig. 1C). In addition to Notch/Wnt signalling, the cellular stress response and fatty acid metabolism were increased, together with metabolomic processes involving dopamine, glucose import metabolism, protein glycosylation, and NAD+/nucleotide biosynthesis. For the 359 downregulated genes in SLE, no significant biological processes were identified.

Regarding the fluidic macroenvironment, the hydroxychloroquine peak was significantly higher in both SLE plasma and urine analyses, which was expected because most patients (76.6%) received antimalarial drugs. Furthermore, upregulation of the peak signals annotated as indole-3-propionic acid/indole-3-methyl acetate and lysophospholipid compounds was found in the plasma, and peak signals with a significantly upregulated intensity including cytidine and 2' Deoxyuridine were found in the urine (Fig. 1D and Table S3). These findings are consistent with the changes in nucleotide metabolism and cellular response to lipids observed in the whole-blood transcriptome.

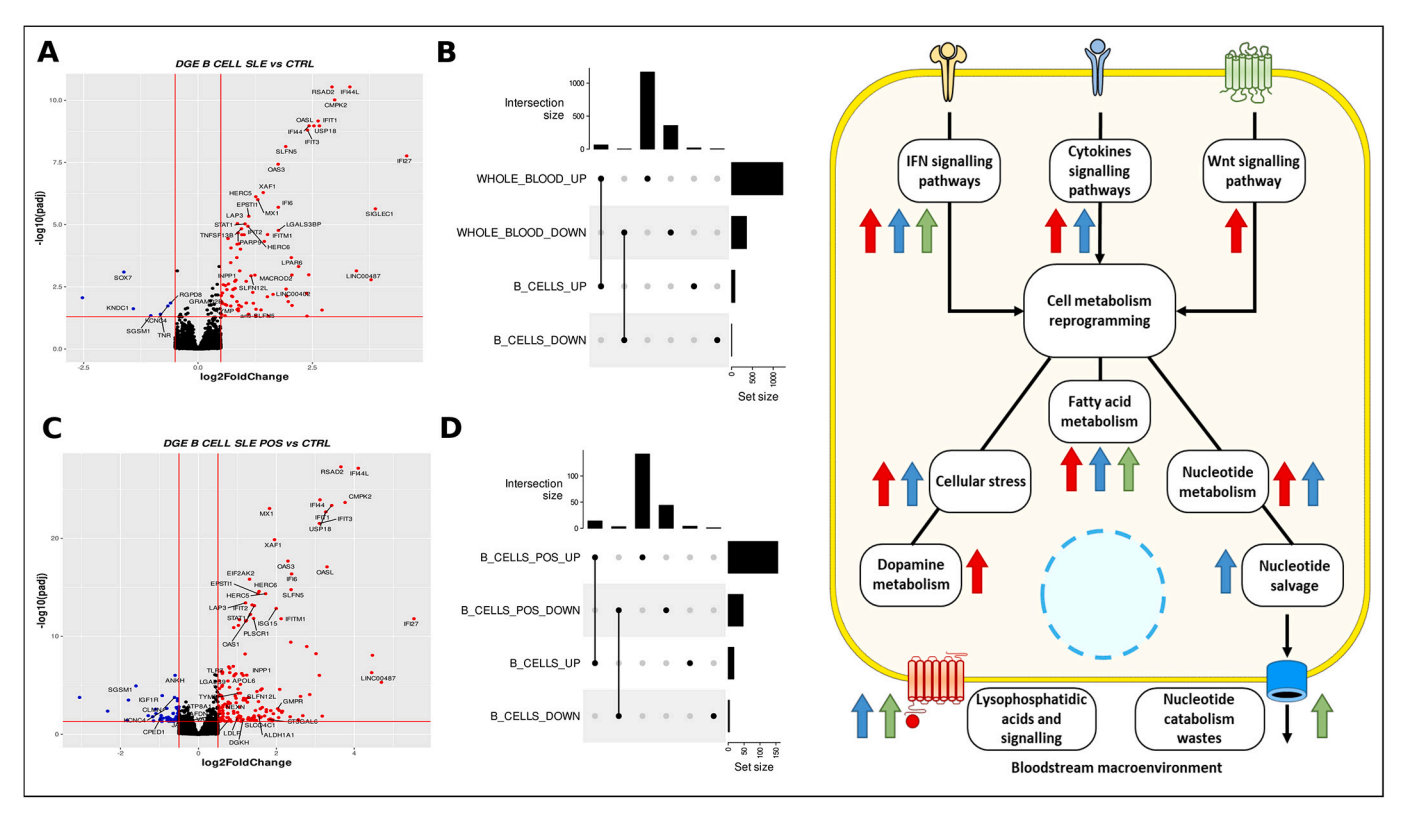


Fig. 2. Identification of unshared systemic lupus erythematosus (SLE) B cell characteristics and interferon (IFN)-α-positive SLE B cell features. A) Volcano plot of the differential gene expression (DGE) analysis of B cells of all patients with SLE vs control samples (CTRL) in the PRECISESADS dataset. The downregulated and upregulated genes are shown in blue and red, respectively. The top 25 upregulated and top 7 downregulated genes are indicated. The threshold of significances, represented as red lines, are |Log2FC| > 0.5 and p.adj < 0.05. B) UpSet plot shows a set size, from top to bottom, of the genes upregulated (UP) and downregulated (DOWN) in the whole blood (WHOLE_BLOOD), and those UP and DOWN in the SLE B cells (B_CELLS). The intersection size, from left to right, identified the shared UP genes, shared DOWN genes, unshared DOWN genes between whole blood and B cells. C) Volcano plot of the DGE analysis of B cells in IFN-α-positive patients with SLE vs CTRL samples in the PRECISESADS dataset. D) UpSet plot shows a set size, from top to bottom, of UP and DOWN genes in the IFN-α-positive SLE B cells (B_CELLS_POS), with 26 upregulated genes and 4 downregulated genes exclusive in all SLE B cells. The intersection size, from left to right, identified the shared UP genes, shared DOWN genes, unshared UP genes and unshared DOWN genes between IFN-α-positive SLE B cells and all B cells. E) Graphical representation of intra-cellular signalling and metabolism pathways and their connection in association with metabolic changes in the macroenvironment. Red arrows indicate an increase in whole blood transcriptomics, blue arrows an increase in B-cell transcriptomics and green arrows an increase in serum and urine metabolomics. (For interpretation of the references to colour in this figure legend, the reader is referred to the web version of this article.)

3.2. Exploration of B cell characteristics

The DGE analysis of the SLE B-cell transcriptome in comparison with CTRL revealed 87 upregulated and 7 downregulated genes (Fig. 2A). GSEA suggested activation of the interferon pathway and immune system, also identified in the EnrichR [18] analysis (results not shown). Among the upregulated genes, were identified thymidine phosphorylase (TYMP) and cytidine/uridine monophosphate kinase 2 (CMPK2) involved in the pyrimidine and purine salvage pathways, respectively. RSAD2, an enzyme involved in viral-induced nucleotide depletion (CTP, UTP) [25] was also detected. Furthermore, LPAR6 a gene encoding the lysophosphatidic acid (LPA) receptor and INPP1 a gene required for LPA signalling and synthesis [26] were revealed. Finally, the long noncoding RNA, LINCO0487, was identified. No enrichment was detected for the downregulated genes.

Differences in the whole-blood transcriptome between SLE and CTRL were compared with the changes found in the B-cell transcriptome. Overall, 65 upregulated and 3 downregulated genes were common in both DGE analyses. Interestingly, 22 genes were found upregulated and 4 genes downregulated in B cell DGE analysis but not in whole-blood DGE analysis (Fig. 2B). For clarity purposes, these genes will be named "unshared" for the rest of the manuscript. Among the unshared upregulated genes, LPAR6 and INPP1 were identified, as well as GRAMD2B, MACROD2, and LINCO0402, which are involved in autoimmunity [27]. Furthermore, Schlafen family members SLFN12L and

SLFN5, and its anti-sense ENSG00000266947 were specifically highlighted in SLE B cells.

3.3. Induction of differential expression of B cell genes by interferon- α

Because IFN- α drives key metabolic changes within the immune cells [28], patients were classified using IFN- α Z-score into IFN- α -positive and IFN- α -negative subgroups to examine how IFN- α regulates the unshared B cell characteristics in SLE.

DGE analysis on 7 IFN- α -negative SLE compared to 22 CTRLs provided only 2 genes differentially expressed, SIRPB1 (log2FC = 1.19 p. adj = 0.0023) and Y_RNA (log2FC = -23.32 p.adj = 2.18e-06), where the latter was not relevant because only expressed in 5 CTRL samples.

DGE analysis of the 22 IFN- α -positive SLE against the 22 CTRLs showed a total of 163 upregulated and 52 downregulated genes (Fig. 2C). As expected, GSEA highlighted interferon signalling pathways (GO:0034340; p.adj = 5.51e-04) and immune system processes (GO:0002702; p.adj = 0.0074) among the upregulated genes. Nucleotide catabolic processes (GO:0006213; p.adj = 0.044 and GO:0009151; p.adj = 0.022) were also enriched. Upregulation of the pyrimidine and purine salvage pathway genes *TYMP*, *CMPK2*, adenosine deaminase (*ADA*), and guanosine monophosphate reductase (*GMPR*) was observed. The urate transporter *LGALS9*, which removes nucleotide degradation metabolites, was also identified. Furthermore, *RSAD2* together with glycosylation enzyme genes e.g. *ST3GAL6*, as hypothesized in other

publications [29] were detected. Lipidic uptake and mobility genes *LDLR*, *APOL6*, *SLCO4C1*, and *ATP8A1* as well as genes encoding specific biosynthetic lipidic class enzymes (*ALDH1A1*, *DGKH*, and *CERS6*) were revealed. *INPP1*, *MOXD1* involved in dopamine metabolism, and Schlafen family members *SLFN12L* and *SLFN5* were also upregulated. The 52 downregulated genes were not enriched in any process.

Of the 22 unshared upregulated genes in the entire SLE cohort, 17 genes were common with the upregulated genes in IFN-α-positive patients. Among them, *IFITM2* and *STAT4* induced by IFN-α, *GRAMD2B*, *MACROD2*, *LINC00402*, *INPP1*, *SLFN5*, *BFSP2*, *EPB41L3*, *NOD2*, *PLCL1*, *RNF144A*, *STOM*, and *UBASH3B* were identified. The remaining five (non-overlapping) upregulated genes were *LPAR6*, *RCBTB2*, *SHLD2P3*, *UPF3AP2*, and *ENSG00000271127*. Of the 4 unshared downregulated genes in the entire SLE cohort, *KCNC4*, *RGPD8*, and *SGSM1* were shared, and *KNDC1* was not shared (Fig. 2D). Findings in whole blood and B cells are summarized in Fig. 2E.

3.4. Validation of total and unshared B cell characteristics in patients

The DGE of the validation dataset revealed 428 upregulated and 144 downregulated genes. The GSEA confirmed the activation of the IFN pathway and immune system as well as nucleoside metabolic processes. Consistent with the PRECISESADS dataset, no enrichment was detected for the set of downregulated genes. Sixty-three genes were found to be upregulated in both datasets, including nucleotide salvage pathway-related genes *TYMP* and *CMPK2*, and *LPAR6*, *SLFN12L*, *SLFN5* and *LINC00487*, but none of the downregulated genes was validated (Fig. S3A)

Of the 22 unshared genes upregulated in B cells from the PRE-CISESADS dataset (Fig. 2B), only 6 were validated: *STAT4*, *LPAR6*, *SLFN5*, NOD2, *EPB41L3* and *STOM*. The differences in the DEGs between the PRECISESADS and the validation datasets may have arisen because of technical and biological consideration such as differences in library preparation, library type, sequencing depth or sample heterogeneity.

Because the validation dataset also classifies the patients with SLE into IFN- α -positive and IFN- α -negative subgroups, a DGE analysis was performed. In total, 92 upregulated genes and one downregulated gene (*EML6*) were common with the PRECISESADS dataset (Fig. S3B). As expected, most of the upregulated validated genes (49 out of 92) were related to the IFN- α response. Finally, the nucleotide salvage pathway-related genes *TYMP*, *CMPK2* and *GMPR*; the urate transporter *LGALS9*; and the LPA synthesis-related *INPP1* were also identified. Additionally, the robustness of nucleotide salvage, dopamine, glycosylation and other pathways in classifying CTRL and IFN- α -positive SLE B cells were confirmed using the XGBoost machine learning method in both PRE-CISESADS and validation datasets (Fig. S4).

3.5. Multi-omics systemic lupus erythematosus data integration

MOFA is a multi-omics integration tool that facilitates the joint analysis of the different -omics layers, such as transcriptomics and metabolomics data (Fig. S5A) to identify the common sources of variation among them, as explained in the material and methods. This approach identifies factors that separate patients with SLE from CTRL individuals and investigates the contributors of these factors to characterize their biological identity. Each factor highlights different altered processes in SLE, which here are split up to ease the understanding and the exploration of the disease. First, the model that identified 18 factors was confirmed to have the best performance in separating the SLE and CTRL samples (Fig. S5B). Because MOFA facilitates the analysis of the direct contribution of genes and metabolomic peaks to each factor, these factors can be characterised. The total metabolomic contribution was lower than the total transcriptomic contribution (Fig. 3A and Table S4). This may be because of the lower suitability of metabolomics data for linear models, higher noise in the data, or a reduced number of features (Fig. S5A). Nonetheless, unsupervised MOFA identified Factors 2, 4, 5,

and 9 (Fig. 3B) as significant in discriminating patients with SLE from CTRLs, with Factor 4 performing better than others (Table S4 and Fig. 3C, D). For Factors 4 and 9, higher factor values were associated with SLE. Therefore, genes or metabolomic peaks positively contributing to these factors support the biological processes underlying the factors, whereas those that contribute negatively contradict these processes. In the case of Factors 2 and 5, patients with SLE present lower values than CTRLs, thus features contributing to the disease are negatively associated with the factor. The identities of the contributors and the biological interpretation of the significant factors are reported in Table 3 and Table S5.

To better understand the biological processes, the significant Factors 2, 4, 5, and 9 were correlated with 49 autoantibodies, 50 clinical measurements and 157 other clinical variables and symptoms (Table S6). Factor 2 showed no association with any clinical feature except for a positive correlation with the age of SLE diagnosis. Factor 5 showed an association with puffy fingers. Factor 9 did not show any significant correlations. Factor 4 was positively correlated with ENA, U1 RNP, Ro52, Ro60, SSA, SM, Jo1, and SSB autoantibodies and with Kappa light chain fragments. Moreover, Factor 4 was positively correlated with the IFN-α Kirou score and IFN-induced cytokines IP 10, IL-1RA, and MCP2, with the exception of IL-1RII, which was negatively correlated.

4. Discussion

The present study aimed to provide an overview of the cellular macroenvironment, through analysis of the whole-blood transcriptome, and fluidic macroenvironment, thanks to analysis of plasma and urine metabolomics, of the SLE B cells that may contribute to their dysfunction. The common changes in the SLE environment and B-cell transcriptome are summarized in Table 4. Although the SLE PRECISESADS cohort had a heterogeneous variety of co-administration of drugs, this work always granted group comparisons having similar percentages in treatments, where possible, focussing on the B cells (Table S7). This approach reduced the effect of drugs on the results.

The whole-blood transcriptome describes the macroenvironment in patients with SLE in which the immune cells are affected by oxidative stress [37] and are forced to import [38] and synthesise lipids [39] to sustain the inflammation. The IFN- α and other cytokine signalling pathways are also activated, leading to an increased influx of and demand for glucose [40]. The DGE analysis between the CTRL and IFN- α -positive SLE samples showed that these processes are exacerbated, including NAD+ metabolism, the pentose phosphate pathway, and serine/aromatic amino acid metabolism (not shown).

The transcriptome of B cells from IFN- α -negative patients with SLE did not differ from that of CTRL B cells, as observed in other studies [7], but supports the limited impact of the treatments in the data. On the other hand, the B-cell transcriptome from IFN- α -positive patients with SLE showed upregulated IFN and cytokine signatures, as expected, in addition to upregulated lipid synthesis and transport [41].

IFN- α -dependent tryptophan physiologically prevents viral proliferation. It is mainly observed in the whole-blood transcriptome of IFN- α -positive patients with SLE, where it is driven by protein translation (WARS1), NAD+ (KYNU, IDO1, PITGS, NNMT, NMNAT2, NAMPT), indole derivatives (IL4I1 [42], AOC1, AOX1) and serotonin (MAOA) synthesis. This finding supports the enrichment of the serotonin metabolic pathway in IFN- α -positive patients observed in GSEA.

Moreover, IFN- α induces a higher demand for nucleotides to sustain cell proliferation during infection, which is fulfilled through de novo synthesis [43]. To face high nucleotide consumption, the nucleotide salvage pathway is activated, recycling nucleotides and preventing excessive energy and time expenditure. Impairment of the nucleotide salvage pathway in lymphocytes leads to low survival and proliferation [44]. *CMPK2* and *TYMP*, associated with the nucleotide salvage pathway, were upregulated in whole blood and B cells of patients, whereas *ADA*, *GMPR*, and *LGALS9* were exclusively upregulated in SLE

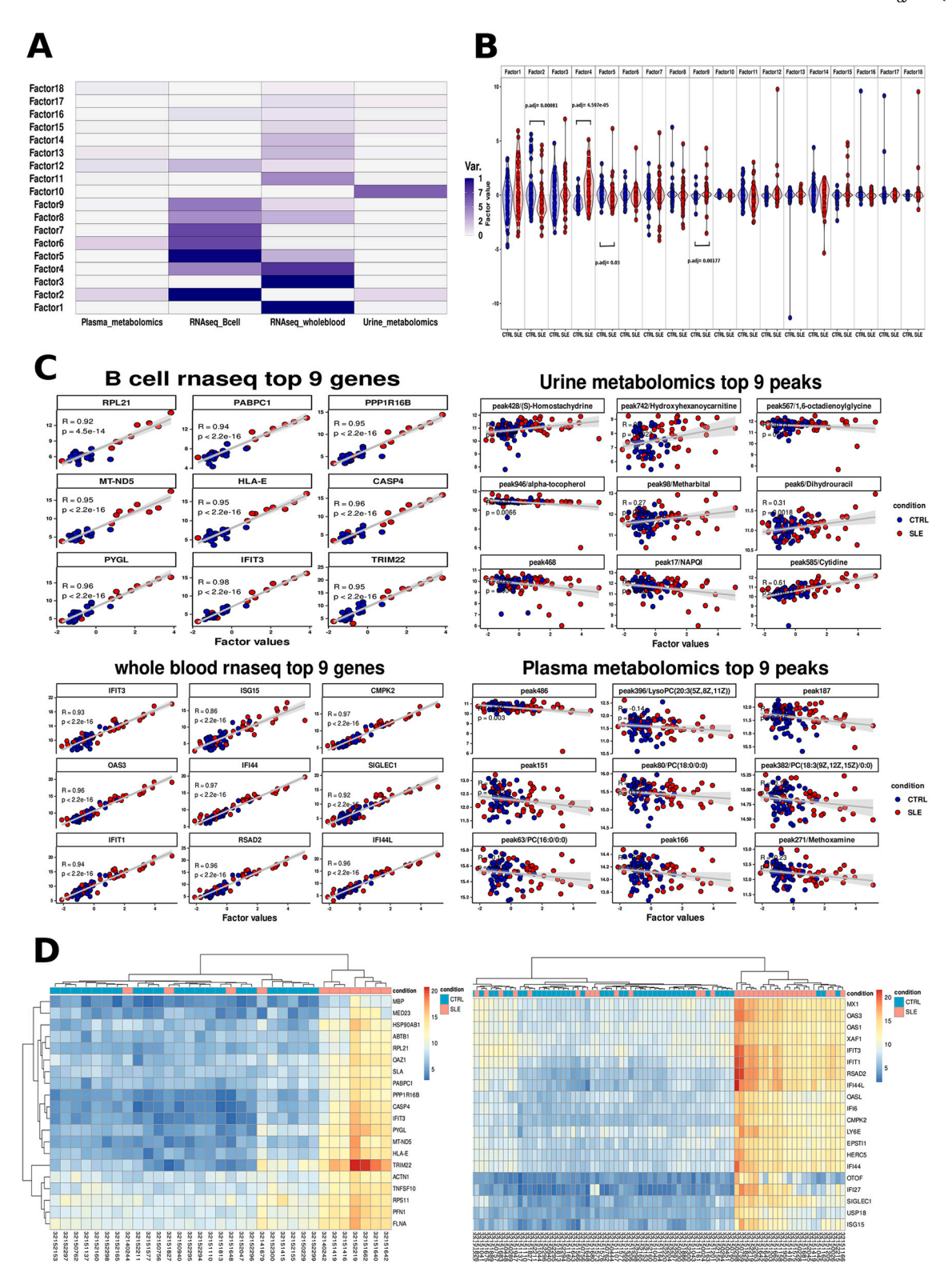


Fig. 3. Identification of variation among multi-omics data from systemic lupus erythematosus (SLE) patients using Multi-Omics Factor Analysis (MOFA) factors. A) The violet scale represents the percentage of variance explained by MOFA factors within an -omics dataset (B-cell transcriptome, whole-blood transcriptome, plasma metabolome, and urine metabolome). The higher the percentage of variance explained among the -omics datasets, the higher the shared variability. B) Violin plot representing SLE (red) and control sample (CTRL; blue) distribution based on each MOFA factor's value. C) Scatterplot of the top 9 genes contributing to Factor 4 in B-cell transcriptome (top left) and in whole-blood transcriptome (bottom left) and top 9 peaks contributing to Factor 4 in urine metabolome (top right) and in plasma metabolome (bottom right). D) Heatmaps using the top 20 genes in B-cell transcriptome (left) and in whole-blood transcriptome (right) contributing to Factor 4. On the top of the heatmaps, blue and red squares identify CTRL and patients with SLE, respectively. Heatmap distance: "Euclidean", clustering method "complete". The gene expression was normalised using the variance stabilising transformation (VST) method. (For interpretation of the references to colour in this figure legend, the reader is referred to the web version of this article.)

Table 3Biological processes of significant MOFA factors and significant contributors.

MOFA Factor	Contribution	Whole-blood transcriptome	B-cell transcriptome	Plasma metabolome	Urine metabolome
Factor 2	+	≻ 0 genes ≻ None	➤ 198 genes ➤ apoptosis (R-HSA-5357801; p.adj = 0.002849), (R-HSA-109581; p.adj = 0.003127) ➤ BCR and WNT signalling pathway (R-HSA-168181; p.adj = 0.003127), (R-HSA-195721; p. adj = 0.03238) ➤ RNA processing (R-HSA-8953854; p.adj = 0.001135)	➤ 2 peaks ➤ cortisol	➤ 2 peaks ➤ None
	-	➤ 3 genes ➤ WNT signalling pathway (TNKS2, PPP2R5C)	➤ 51 genes	 ≥ 25 peaks > phosphatidylcholines > sphingomyelins, lysophosphatidic acids > cortisol precursor 11-deoxycortisol > hypertensive drug alphahydroxymetoprolol 	➤ 2 peaks ➤ None
Factor 4	+	➤ 25 genes ➤ interferon (GO:0071357; p.adj = 7.046e-25) ➤ cytokine signalling (GO:0019221; p.adj = 2.267e-12), ➤ pyrimidine biosynthetic process (GO:0009221; p.adj = 0.0176) ➤ IFN-α-induced transcription factor IRF1 (p.adj = 0.006840)	➤ 10 genes ➤ IFN-α (GO:0071357; p.adj = 0.02048) ➤ cytokine signalling (R-HSA-1280215; p.adj = 0.02482) ➤ B-cell activation (GO:0002484; p.adj = 0.03741)	> 1 peak > None	➤ 1 peak ➤ None
	-	➤ 0 genes ➤ None	➤ 0 genes ➤ None	➤ 11 peaks ➤ Lipids phosphatidylcholines, sphingomyelins, and lysophosphatidic acids ➤ hypertensive drug methoxamine	➤ 0 peaks ➤ cytidine

MOFA Factor	Contribution	Whole-blood transcriptome	B-cell transcriptome	Plasma metabolome	Urine metabolome
Factor 5	+	≻ 48 genes	≻ 61 genes	≻ 1 peak	➤ 0 peaks
		➤ hydrogen peroxide catabolic process (GO:0042744; p.adj	➤ apoptotic signalling	➤ None	➤ None
		= 0.000082)	(GO:2001235; p.adj = 0.026)		
		➤ myeloid cell development (GO:0061515; p.adj =	➤ p21 regulation by RUNX3 (R-		
		0.04577)	HSA-8941855 p.adj = 0.032)		
	_	≻ 0 genes	➤ 14 genes	➤ 0 peaks	➤ 2 peaks
		➤ None	➤ minor mRNA maturation process (GO:0006370; p.adj =	➤ None	➤ None
			0.017)		
Factor 9	+	➤ 51 genes	➤ 29 genes	➤ 2 peaks	≻ 1 peak
		 ➤ neutrophil immunity (GO:0002446; p.adj = 2.294e-9) ➤ interleukin signalling pathways (R-HSA-449147; p.adj = 0.006192) (Bioplanet 2019; p.adj = 0.007422), (Bioplanet 2019; p.adj = 0.008916) 	≻ None	➤ None	➤ None
	_	➤ 12 genes	➤ 16 genes	➤ 0 peaks	→ 4 peaks
		\succ interleukin signalling pathways (R-HSA-449147; p.adj = 0.008123), (R-HSA-9020702; p.adj = 0.04983)	➤ None	➤ None	➤ asthma corticosteroid 6- beta-hydroxy-mometasone furoate

Each significant MOFA factor is described in terms of positive (+) and negative (-) contribution. The total number of contributors in each OMICS data set (relevant genes in whole blood and in B cells and relevant peaks in plasma and urine) with the main associated biological pathway (and their p.adj) obtained from the EnrichR analysis are indicated.

IFN- α -positive B cells. Reinforcing the observation of nucleotide depletion, patients showed increased cytidine in the urine. This metabolite is a key contributor to Factor 4 in MOFA and better discriminates SLE and CTRL samples in urine than other factors. Consistent with this finding, the upregulation of *TYMS*, *NT5C3A*, *TYMP*, *DYPS*, and *UPB1* in the whole-blood transcriptome of IFN- α -positive patients clearly suggests an upregulation of thymidine/uridine degradation toward valine-leucine metabolism, and the upregulated cytidine deaminase suggests cytidine degradation. The environmental depletion of nucleotides is supported by the upregulation of *RSAD2* in whole blood and B cells, which is a major contributor among the whole blood genes to Factor 4 in MOFA. RSAD2 enzyme drives nucleotide depletion induced by IFN- α signalling

in response to viral infection. It interferes with de novo nucleotide synthesis by collaborating with mitochondrial CMPK2, which supports RSAD2 activity [25]. Treatments specific for de novo nucleotide synthesis are available and used in SLE [45], reducing the flare and autoantibodies in patients. This is consistent with a direct or indirect effect on B cell activity in SLE [46]. The data here suggest an increased nucleotide salvage pathway induced by IFN- α signalling. Nowadays, no treatments affect this pathway, though, from the current findings, this could be a valuable target.

Remarkably, the LPA receptor-encoding *LPAR6* was identified as a common upregulated gene in both B-cell transcriptome and whole-blood transcriptome in SLE. This, together with *INPP1* upregulation, suggests a

Table 4

Metabolic processes upregulated in the systemic lupus erythematosus (SLE) dataset and in the MOFA integration.

Process	B cells	Whole blood	Plasma metabolomics	Urine metabolomics	MOFA integration	Clinical implications
Nucleotide metabolism	Observed	Observed	Not Observed	Observed	Observed Pyrimidine deoxyribonucleotide	Autoimmune events observed in patients with deficiency in the
	Boosted in IFN-α-positive patients	Boosted in IFN-α-positive patients			biosynthetic process enriched in top whole-blood genes contributing to Factor 4 Cytidine, first urine metabolite in factor	nucleotide salvage pathway [30] No cell-specific details available
					2 separation	
Tryptophan metabolism	Not observed	Observed Boosted in IFN-α-positive patients	Observed	Not Observed	Not Observed	Consumption of tryptophan was increased in SLE [31]. It drives the synthesis of the immunoregulator kynurenine [32] Microbiota affect tryptophan metabolism by being involved in physiological processes and
						autoimmunity [33]
Fatty acid mobility/bio- synthesis	Observed Boosted in IFN-α-positive patients	Observed Boosted in IFN-α-positive patients	Not Observed	Not Observed	Observed Phosphatidylcholines and sphingomyelins are top negative plasma contributors in Factors 2 and 4	Increased to sustain the development of inflammatory mediators
Lysophos-	Observed	Observed	Observed	Not Observed	Observed	No information in B cells
phatidic acid signalling	Boosted in IFN-α-positive patients	Boosted in IFN-α-positive patients			Lysophosphatidic acids are top negative plasma contributors in Factors 2 and 4	Suggested to have an immunoregulatory function [34]
Dopamine	Observed Only in IFN- α-positive	Observed Boosted in IFN-α-positive	Not Observed	Not Observed	Not Observed	Novel mediator of the inflammation spotted in PBMCs No detailed cell-specific information i
	patients	patients				available [35]
Glycosylation	Observed Only in IFN-	Observed Boosted in	Not Observed	Not Observed	Not Observed	Alteration in glycosylation identified i PBMCs [36]
	α-positive patients	IFN-α-positive patients				No information in B cells is available
Schlafen protein	Observed Boosted in	Observed Boosted in	Not Observed	Not Observed	Not Observed	Protein with unknown function in th T cells
	IFN-α-positive patients	IFN-α-positive patients				Has not been identified in B cells before

role for LPA in SLE pathogenesis. The intersection between the genes upregulated in SLE and in IFN- α -positive SLE indicated that only *INPP1* is affected by IFN- α . This observation is consistent with the increased lysophospholipids, which bind to and activate LPAR6 on B cells, and validates the restricted upregulation of the LPA receptor LPAR6 in SLE B cells. Moreover, lysophospholipids were among the top negative contributors in Factors 2 and 4 of the MOFA, which separate CTRL and SLE samples. LPAR6 is a novel LPA receptor whose function is not yet known, but similar receptor LPAR5 suggest an immunomodulatory role in B cells and autoimmunity [34].

Protein glycosylation was also altered in SLE [36]. In the whole-blood transcriptome, enrichment in asparagine N-linked and sialic acid glycosylation were found, whereas B cells of IFN- α -positive patients with SLE showed upregulation in glycosylation enzymes such as the sialyltransferase *ST3GAL6*. Recently, our research group validated the protein glycosylation changes within SLE B cells [47]. LINC00487 is a long non-coding RNA associated with Sjogren's syndrome disease activity [48], induced by IFN- α and involved in B cell dysregulation. In the present study, it was found to be upregulated in both PRECISESADS B-cell and whole-blood transcriptome datasets and in B-cell validation dataset. Moreover, in SLE whole blood, it was weakly correlated with the lupus activity score (Pearson correlation coefficient = 0.16, p = 0.0026). This suggests that IFN- α signalling causes an alteration in glycosylation and long non-coding RNA over metabolism [49].

Finally, many Schlafen family members were identified in the present study. These were recently discovered in T cells, but their function remains unclear [50]. In the PRECISESADS and validation B-cell transcriptome datasets from IFN- α -positive patients with SLE, *SLFN5* and *SLFN12L* were upregulated, suggesting for the first time a role of IFN- α in their expression in B cells, as is known for T cells [51].

According to the top genes and metabolomic peaks and the clinical

features highlighted with the MOFA analyses, Factor 4 incorporated the IFN-α changes, observed both in B-cell and whole-blood transcriptome contributors, which were confirmed by the correlation with IFNα-induced cytokine and autoantibody production in clinical data. Factor 2 was linked to inflammation and antigen presentation. It was positively correlated with the diagnosis age of SLE, suggesting a change in these processes driven by age, likely due to the development of autoimmunity. Factor 5 was associated with reactive oxygen species (ROS) catabolism in whole blood, leading to apoptosis and with a reduction in mRNA maturation in B cells. It distinguishes patients with puffy fingers (dactylitis), suggesting a direct or indirect stress-oxidative role in this inflammation. Factor 9 was linked to interleukin and neutrophil inflammation in whole blood, without associations with clinical data. Overall, MOFA factors caught different aspects of the disease and isolated them. MOFA provided a way to identify, biological changes and clinical events driven by the same altered process, such as interferon (Factor 4), physiological antigen recognition (Factor 2), stress (Factor 5) and neutrophils (Factor 9). Among the described factors, the 4th was related to patients with the worst prognosis, as high levels of Factor 4 were correlated to higher levels of autoantibodies and more severe disease. Factor 5 linked the ROS production in whole blood with the puffy fingers, suggesting that ROS are mechanism by which stress can lead to this clinical inflammation, as already previously suspected [52].

To our knowledge, this is the first exploratory analysis that attempted to integrate the omics data of SLE using MOFA. Limitation of this study included the low MOFA efficiency in catching biological variability when exploring metabolomics data, that are not naturally linear. It favors transcriptomics contribution in the results, excluding the majority of the metabolomics variability in MOFA factors. Further experiments targeting enzymes and receptors within the identified pathway are required to elucidate the exact role of lysophosphatidic-acid

signalling, glycosylation, and nucleotide salvage pathway changes in SLE. It is noteworthy that this study represents a novel approach to the investigation of SLE but also autoimmune diseases using multiple sources of OMICS data, having the potential to provide a comprehensive explanation of the underlying changes in the diseases.

Supplementary data to this article can be found online at https://doi.org/10.1016/j.clim.2024.110243.

PRECISESADS Flow Cytometry Study Group

Montserrat Alvarez⁸, Damiana Alvarez-Errico⁹, Nancy Azevedo¹⁰, Nuria Barbarroja¹¹, Anne Buttgereit¹², Qingyu Cheng¹³, Carlo Chizzolini⁸, Jonathan Cremer¹⁴, Aurélie De Groof¹⁵, Ellen De Langhe¹⁶, Julie Ducreux¹⁵, Aleksandra Dufour⁸, Velia Gerl¹³, Maria Hernandez-Fuentes¹⁷, Laleh Khodadadi¹³, Katja Kniesch¹⁸, Tianlu Li⁹, Chary Lopez-Pedrera¹¹, Zuzanna Makowska¹², Concepción Marañón³, Brian Muchmore³, Esmeralda Neves¹⁰, Bénédicte Rouvière¹, Quentin Simon¹, Elena Trombetta¹⁹, Nieves Varela³ & Torsten Witte¹⁸

⁸Immunology and Allergy, University Hospital and School of Medicine, Geneva, Switzerland.

⁹Chromatin and Disease Group, Bellvitge Biomedical Research Institute (IDIBELL), Barcelona, Spain.

 10 Serviço de Imunologia EX-CICAP, Centro Hospitalar e Universitário do Porto, Porto, Portugal.

 11 IMIBIC, Reina Sofia Hospital, University of Cordoba, Córdoba, Spain.

¹²Bayer AG, Berlin, Germany.

¹³Department of Rheumatology and Clinical Immunology, Charité University Hospital, Berlin, Germany.

 14 Laboratory of Clinical Immunology, Department of Microbiology and Immunology, KU Leuven, Leuven, Belgium.

¹⁵Pôle de Pathologies Rhumatismales Inflammatoires et Systémiques, Institut de Recherche Expérimentale et Clinique, Université Catholique de Louvain, Brussels, Belgium.

¹⁶Division of Rheumatology, University Hospitals Leuven and Skeletal Biology and Engineering Research Center, KU Leuven, Leuven, Belgium.

¹⁹Laboratorio di Analisi Chimico Cliniche e Microbiologia - Servizio di Citofluorimetria, Fondazione IRCCS Ca' Granda Ospedale Maggiore Policlinico di Milano, Milan, Italy.

PRECISESADS Clinical Consortium

Rocío Aguilar-Quesada²⁰, Maria Angeles Aguirre-Zamorano²¹, Isabel Almeida²², Niklas Baerlecken¹⁸, Attila Balog²³, Doreen Belz²⁴, Lorenzo Beretta²⁵, Ricardo Blanco Alonso²⁶, Márta Bocskai²³, Mariana Brandão²², José Luis Callejas Rubio²⁷, Ana Campar²², Maria-Carmen Castro-Villegas²¹, Ricard Cervera²⁸, Eduardo Collantes²¹, Divi Cornec²⁹, Alfonso Corrales Martínez²⁶, Magdolna Deák²³, Valérie Devauchelle-Pensec²⁹, Sonja Dulic²³, Alejandro Escudero-Contreras²¹, Gerard Espinosa²⁸, Raquel Faria²², Fátima Farinha²², María Concepción Fernández Roldán²⁷, Tania Gomes Anjos³, Miguel A. González-Gay²⁶, Falk Hiepe³⁰, Nicolas Hunzelmann²⁴, Sandrine Jousse-Joulin²⁹, Gabriella Kádár²³, Laszló Kovács²³, Bernard Lauwerys³¹, Michaela Lehner³², Antonio López-Berrio²⁰, Rik Lories³³, António Marinho²², Jacqueline Marovac¹⁷, Pier Luigi Meroni³⁴, Blanca Miranda³⁰, Immaculada Jiménez Moleón²⁷, Héctor Navarro-Linares²⁰, Rafaela Ortega-Castro²¹, Norberto Ortego²⁷, Enrique Ramón Garrido³⁵, Enrique Raya²⁷, Raquel Ríos Fernández²⁷, Ignasi Rodríguez-Pintó²⁸, Alain Saraux²⁹, Georg Stummvoll³², Carlos Vasconcelos²² & Michael Zauner³²

¹⁷UCB, Slough, UK.

¹⁸Klinik für Immunologie Und Rheumatologie, Medical University Hannover, Hannover, Germany.

²⁰Andalusian Public Health System Biobank, PTS Granada, Granada, Spain.

²¹Hospital Universitario Reina Sofía Andaluz de Salud, Córdoba,

Spain

²²Centro Hospitalar do Porto, Porto, Portugal.

²³University of Szeged, Szeged, Hungary.

²⁴Klinikum Der Universitaet Zu Koeln, Cologne, Germany.

²⁵Fondazione IRCCS Ca Granda Ospedale Maggiore Policlinico, Milan, Italy.

²⁶Hospital Universitario Marqués de Valdecilla, Servicio Cántabro de Salud, Santander, Spain.

²⁷Hospital Universitario San Cecilio, Servicio Andaluz de Salud, Granada, Spain.

²⁸Hospital Clinic, Institut D'Investigacions Biomèdiques August Pi i Sunyer, Barcelona, Catalonia, Spain.

²⁹Centre Hospitalier Universitaire de Brest, Hopital de La Cavale Blanche, Brest, France.

³⁰Deutsches Rheuma-Forschungszentrum Berlin, Berlin, Germany,

³¹Université Catholique de Louvain, Louvain, Belgium.

³²Medizinische Universitat Wien, Vienna, Austria.

³³Katholieke Universiteit Leuven, Leuven, Belgium.

³⁴Università Degli Studi di Milano, Milan, Italy.

³⁵Hospital Regional de Málaga, Servicio Andaluz de Salud, Málaga,

Grant

Innovative Medicines Initiative Joint Undertaking (Grant Agreement #115565).

Declaration of Generative AI and AI-assisted technologies in the writing process

During the writing and editing of this manuscript, any AI tool or program was used.

CRediT authorship contribution statement

Cristian Iperi: Writing - original draft, Validation, Software, Methodology, Investigation, Formal analysis. Álvaro Fernández-Ochoa: Writing - review & editing, Software, Methodology, Data curation. Jacques-Olivier Pers: Writing – review & editing, Resources, Project administration, Funding acquisition. Guillermo Barturen: Writing – review & editing, Resources, Project administration, Funding acquisition. Marta Alarcón-Riquelme: Writing – review & editing. Resources, Project administration, Funding acquisition, Rosa Ouirantes-Piné: Writing - review & editing, Data curation. Isabel Borrás-Linares: Writing - review & editing, Data curation. Antonio Segura-Carretero: Writing - review & editing, Resources, Project administration, Funding acquisition. Divi Cornec: Writing - review & editing, Resources, Project administration, Funding acquisition. Anne Bordron: Writing - review & editing, Supervision, Methodology, Funding acquisition. Christophe Jamin: Writing - review & editing, Supervision, Methodology, Funding acquisition.

Declaration of competing interest

The authors have declared that no conflict of interest exists.

Data and code availability

All data included in our study were analysed in R and are available upon request at ELIXIR Luxemburg, with the permanent link: doi:10.17881/th9v-xt85. Code is available at https://github.com/IxI-97/SLE_PRECISESADS.

Acknowledgments

The research leading to these results has received support from the

Innovative Medicines Initiative Joint Undertaking under Grant Agreement Number 115565, resources of which are composed of financial contributions from the European Union's Seventh Framework Program (FP7/2007–2013) and EFPIA companies in-kind contributions. We would like to acknowledge 3TR and the PRECISESADS consortium, which guaranteed the availability of the data used in this article and the opportunity to analyse them. A special thanks to the Italian journalist and scientific communicator Piero Angela, for inspiring the new researcher generation to stay curious. These are the fruits of his love for science. CI was funded by the Université de Brest and the Région Bretagne.

References

- E. Nashi, Y. Wang, B. Diamond, The role of B cells in lupus pathogenesis, Int. J. Biochem. Cell Biol. 42 (2010) 543–550, https://doi.org/10.1016/j. biocel.2009.10.011.
- [2] B. Dema, N. Charles, Autoantibodies in SLE: specificities, isotypes and receptors, Antibodies. 5 (2016) 2, https://doi.org/10.3390/antib5010002.
- [3] O.T.M. Chan, L.G. Hannum, A.M. Haberman, M.P. Madaio, M.J. Shlomchik, A novel mouse with B cells but lacking serum antibody reveals an antibodyindependent role for B cells in murine lupus, J. Exp. Med. 189 (1999) 1639–1648.
- [4] C. Iperi, A. Bordron, M. Dueymes, J.-O. Pers, C. Jamin, Metabolic program of regulatory B lymphocytes and influence in the control of malignant and autoimmune situations, Front. Immunol. 12 (2021) 735463, https://doi.org/ 10.3389/fimmu.2021.735463.
- [5] V. Oke, I. Gunnarsson, J. Dorschner, S. Eketjäll, A. Zickert, T.B. Niewold, et al., High levels of circulating interferons type I, type II and type III associate with distinct clinical features of active systemic lupus erythematosus, Arthritis Res. Ther. 21 (2019) 107, https://doi.org/10.1186/s13075-019-1878-y.
- [6] G. Barturen, S. Babaei, F. Català-Moll, M. Martínez-Bueno, Z. Makowska, J. Martorell-Marugán, et al., Integrative analysis reveals a molecular stratification of systemic autoimmune diseases, Arthritis Rheumatol. Hoboken NJ. 73 (2021) 1073–1085, https://doi.org/10.1002/art.41610.
- [7] Á. Fernández-Ochoa, C. Brunius, I. Borrás-Linares, R. Quirantes-Piné, M. de la L. Cádiz-Gurrea, null Precisesads Clinical Consortium, M.E. Alarcón Riquelme, A. Segura-Carretero, Metabolic disturbances in urinary and plasma samples from seven different systemic autoimmune diseases detected by HPLC-ESI-QTOF-MS, J. Proteome Res. 19 (2020) 3220–3229, https://doi.org/10.1021/acs. iproteome.0c00179.
- [8] N. Kedia-Mehta, D.K. Finlay, Competition for nutrients and its role in controlling immune responses, Nat. Commun. 10 (2019) 2123, https://doi.org/10.1038/ e41467.019.10015.4
- [9] B. Panwar, B.J. Schmiedel, S. Liang, B. White, E. Rodriguez, K. Kalunian, et al., Multi-cell type gene coexpression network analysis reveals coordinated interferon response and cross-cell type correlations in systemic lupus erythematosus, Genome Res 31 (2021) 659–676, https://doi.org/10.1101/gr.265249.120.
- [10] M.C. Hochberg, Updating the American College of Rheumatology revised criteria for the classification of systemic lupus erythematosus, Arthritis Rheum. 40 (9) (1997) 1725, https://doi.org/10.1002/art.178040092.
- [11] A. Dobin, C.A. Davis, F. Schlesinger, J. Drenkow, C. Zaleski, S. Jha, et al., STAR: ultrafast universal RNA-seq aligner, Bioinformatics. Oxf. Engl. 29 (2013) 15–21, https://doi.org/10.1093/bioinformatics/bts635.
- [12] B. Li, Dewey CN.RSEM: accurate transcript quantification from RNA-Seq data with or without a reference genome, BMC Bioinformatics. 12 (2011) 323, https://doi. org/10.1186/1471-2105-12-323.
- [13] E. Becht, N.A. Giraldo, L. Lacroix, B. Buttard, N. Elarouci, F. Petitprez, et al., Estimating the population abundance of tissue-infiltrating immune and stromal cell populations using gene expression, Genome Biol. 17 (2016) 218, https://doi.org/ 10.1186/s13059-016-1070-5.
- [14] C.B. Steen, C.L. Liu, A.A. Alizadeh, A.M. Newman, Profiling cell type abundance and expression in bulk tissues with CIBERSORTx, Methods Mol. Biol. Clifton NJ. 2117 (2020) 135–157, https://doi.org/10.1007/978-1-0716-0301-7-7.
- [15] K.A. Kirou, C. Lee, S. George, K. Louca, M.G.E. Peterson, M.K. Crow, Activation of the interferon-alpha pathway identifies a subgroup of systemic lupus erythematosus patients with distinct serologic features and active disease, Arthritis Rheum. 52 (2005) 1491–1503, https://doi.org/10.1002/art.21031.
- [16] Z. Gu, R. Eils, M. Schlesner, Complex heatmaps reveal patterns and correlations in multidimensional genomic data, Bioinformatics. 32 (2016) 2847–2849, https:// doi.org/10.1093/bioinformatics/btw313.
- [17] M.I. Love, W. Huber, S. Anders, Moderated estimation of fold change and dispersion for RNA-seq data with DESeq2, Genome Biol. 15 (2014) 550, https:// doi.org/10.1186/s13059-014-0550-8.
- [18] A. Subramanian, P. Tamayo, V.K. Mootha, S. Mukherjee, B.L. Ebert, M.A. Gillette, et al., Gene set enrichment analysis: a knowledge-based approach for interpreting genome-wide expression profiles, Proc. Natl. Acad. Sci. 102 (2005) 15545–15550, https://doi.org/10.1073/pnas.0506580102.
- [19] E.Y. Chen, C.M. Tan, Y. Kou, Q. Duan, Z. Wang, G.V. Meirelles, et al., Enrichr: interactive and collaborative HTML5 gene list enrichment analysis tool, BMC Bioinformatics. 14 (2013) 128, https://doi.org/10.1186/1471-2105-14-128.
- [20] A. Gil de la Fuente, J. Godzien, M. Fernández López, F.J. Rupérez, C. Barbas, A. Otero, Knowledge-based metabolite annotation tool: CEU mass mediator,

- J. Pharm. Biomed. Anal. 154 (2018) 138–149, https://doi.org/10.1016/j.jpba.2018.02.046.
- [21] CMMR CEU Mass Mediator API in R. https://github.com/cran/cmmr, 2019 (accessed August 20, 2022).
- [22] D.S. Wishart, D. Tzur, C. Knox, R. Eisner, A.C. Guo, N. Young, et al., HMDB: the human metabolome database, Nucleic Acids Res. 35 (2007) D521–D526, https:// doi.org/10.1093/nar/gkl923.
- [23] M. Wang, J.J. Carver, V.V. Phelan, L.M. Sanchez, N. Garg, Y. Peng, et al., Sharing and community curation of mass spectrometry data with GNPS, Nat. Biotechnol. 34 (2016) 828–837, https://doi.org/10.1038/nbt.3597.
- [24] R. Argelaguet, D. Arnol, D. Bredikhin, Y. Deloro, B. Velten, J.C. Marioni, MOFA+: a statistical framework for comprehensive integration of multi-modal single-cell data, Genome Biol. 21 (1) (2020) 111, https://doi.org/10.1186/s13059-020-02015-1.
- [25] K.H. Ebrahimi, D. Howie, J.S. Rowbotham, J. McCullagh, F.A. Armstrong, W. S. James, Viperin, through its radical-SAM activity, depletes cellular nucleotide pools and interferes with mitochondrial metabolism to inhibit viral replication, FEBS Lett. 594 (2020) 1624–1630, https://doi.org/10.1002/1873-3468.13761.
- [26] D.I. Benjamin, S.M. Louie, M.M. Mulvihill, R.A. Kohnz, D.S. Li, L.G. Chan, et al., Inositol phosphate recycling regulates glycolytic and lipid metabolism that drives cancer aggressiveness, ACS Chem. Biol. 9 (2014) 1340–1350, https://doi.org/ 10.1021/cb5001907.
- [27] D. Peltier, M. Radosevich, V. Ravikumar, S. Pitchiaya, T. Decoville, S.C. Wood, et al., RNA-seq of human T cells after hematopoietic stem cell transplantation identifies Linc00402 as a regulator of T cell alloimmunity, Sci. Transl. Med. 13 (2021), https://doi.org/10.1126/scitranslmed.aaz0316 eaaz0316.
- [28] D. Wu, D.E. Sanin, B. Everts, Q. Chen, J. Qiu, et al., Type 1 interferons induce changes in core metabolism that are critical for immune function, Immunity. 44 (2016) 1325–1336, https://doi.org/10.1016/j.immuni.2016.06.006.
- [29] I. Ramos-Martínez, E. Ramos-Martínez, M. Cerbón, A. Pérez-Torres, L. Pérez-Campos Mayoral, M.T. Hernández-Huerta, et al., The role of B cell and T cell glycosylation in systemic lupus erythematosus, Int. J. Mol. Sci. 24 (2023) 863, https://doi.org/10.3390/ijms24010863.
- [30] A.V. Sauer, I. Brigida, N. Carriglio, A. Aiuti, Autoimmune dysregulation and purine metabolism in adenosine deaminase deficiency, Front. Immunol. 3 (2012) 265, https://doi.org/10.3389/fimmu.2012.00265.
- [31] B. Widner, N. Sepp, E. Kowald, S. Kind, M. Schmuth, D. Fuchs, Degradation of tryptophan in patients with systemic lupus erythematosus, Adv. Exp. Med. Biol. 467 (1999) 571–577, https://doi.org/10.1007/978-1-4615-4709-9 71.
- [32] K. Åkesson, S. Pettersson, S. Ståhl, I. Surowiec, M. Hedenström, S. Eketjäll, et al., Kynurenine pathway is altered in patients with SLE and associated with severe fatigue, Lupus Sci. Med. 5 (2018) e000254, https://doi.org/10.1136/lupus-2017-000254.
- [33] E.C. Rosser, C.J.M. Piper, D.E. Matei, P.A. Blair, A.F. Rendeiro, M. Orford, et al., Microbiota-derived metabolites suppress arthritis by amplifying aryl-hydrocarbon receptor activation in regulatory B cells, Cell Metab. 31 (2020) 837–851.e10, https://doi.org/10.1016/j.cmet.2020.03.003.
- [34] J. Hu, S.K. Oda, K. Shotts, E.E. Donovan, P. Strauch, L.M. Pujanauski, et al., Lysophosphatidic Acid (LPA) receptor 5 inhibits B cell antigen receptor signaling and antibody response, J. Immunol. Baltim. Md. 1950 (193) (2014) 85–95, https:// doi.org/10.4049/ijmmunol.1300429.
- [35] M. Jafari, G. Ahangari, M. Saberi, S. Samangoui, R. Torabi, M. Zouali, Distorted expression of dopamine receptor genes in systemic lupus erythematosus, Immunobiology. 218 (2013) 979–983, https://doi.org/10.1016/j. imbio.2012.11.002.
- [36] I. Alves, B. Santos-Pereira, H. Dalebout, S. Santos, M.M. Vicente, A. Campar, M. Thepaut, F. Fieschi, et al., Protein mannosylation as a diagnostic and prognostic biomarker of lupus nephritis: an unusual glycan neoepitope in systemic lupus erythematosus, Arthritis Rheumatol. Hoboken NJ. 73 (2021) 2069–2077, https://doi.org/10.1002/art.41768.
- [37] A. Perl, Oxidative stress in the pathology and treatment of systemic lupus erythematosus, Nat. Rev. Rheumatol. 9 (2013) 674–686, https://doi.org/10.1038/ nrrheum.2013.147.
- [38] M.J. Hubler, A.J. Kennedy, Role of lipids in the metabolism and activation of immune cells, J. Nutr. Biochem. 34 (2016) 1–7, https://doi.org/10.1016/j. inutbio.2015.11.002.
- [39] X. Qian, Z. Yang, E. Mao, E. Chen, Regulation of fatty acid synthesis in immune cells, Scand. J. Immunol. 88 (2018) e12713, https://doi.org/10.1111/sji.12713.
- [40] C.S. Palmer, M. Ostrowski, B. Balderson, N. Christian, S.M. Crowe, Glucose metabolism regulates T cell activation, differentiation, and functions, Front. Immunol. 6 (2015). https://www.frontiersin.org/articles/10.3389/fimmu.2015. 00001 (accessed August 18, 2022).
- [41] L.R. Waters, F.M. Ahsan, D.M. Wolf, O. Shirihai, M.A. Teitell, Initial B cell activation induces metabolic reprogramming and mitochondrial remodeling, iScience. 5 (2018) 99–109, https://doi.org/10.1016/j.isci.2018.07.005.
- [42] X. Zhang, M. Gan, J. Li, H. Li, M. Su, D. Tan, S. Wang, et al., Endogenous indole pyruvate pathway for tryptophan metabolism mediated by IL4I1, J. Agric. Food Chem. 68 (2020) 10678–10684, https://doi.org/10.1021/acs.jafc.0c03735.
- [43] A.C. Allison, T. Hovi, R.W. Watts, A.D. Webster, The role of de novo purine synthesis in lymphocyte transformation, CIBA Found. Symp. (1977) 207–224, https://doi.org/10.1002/9780470720301.ch13.
- [44] O. Choi, D.A. Heathcote, K.-K. Ho, P.J. Müller, H. Ghani, E.W.-F. Lam, P.G. Ashton-Rickardt, S. Rutschmann, A deficiency in nucleoside salvage impairs murine lymphocyte development, homeostasis and survival, J. Immunol. Baltim. Md. 1950 (188) (2012) 3920–3927, https://doi.org/10.4049/jimmunol.1102587.

- [45] R. Sakthiswary, E. Suresh, Methotrexate in systemic lupus erythematosus: a systematic review of its efficacy, Lupus. 23 (2014) 225–235, https://doi.org/ 10.1177/0961203313519159.
- [46] S. Eickenberg, E. Mickholz, E. Jung, J.-R. Nofer, H. Pavenstädt, A.M. Jacobi, Mycophenolic acid counteracts B cell proliferation and plasmablast formation in patients with systemic lupus erythematosus, Arthritis Res. Ther. 14 (2012) R110, https://doi.org/10.1186/ar3835.
- [47] M. Morel, P. Pochard, W. Echchih, M. Dueymes, C. Bagacean, S. Jousse-Joulin, V. Devauchelle-Pensec, et al., Abnormal B cell glycosylation in autoimmunity: a new potential treatment strategy, Front. Immunol. 13 (2022) 975963, https://doi. org/10.3389/fimmu.2022.975963.
- [48] J. Inamo, K. Suzuki, M. Takeshita, Y. Kassai, M. Takiguchi, R. Kurisu, et al., Identification of novel genes associated with dysregulation of B cells in patients with primary Sjögren's syndrome, Arthritis Res. Ther. 22 (2020) 153, https://doi. org/10.1186/s13075-020-02248-2.
- [49] L.B. Giron, F. Colomb, E. Papasavvas, L. Azzoni, X. Yin, M. Fair, et al., Interferon-α alters host glycosylation machinery during treated HIV infection, eBioMedicine. 59 (2020), https://doi.org/10.1016/j.ebiom.2020.102945.
- [50] P. Geserick, F. Kaiser, U. Klemm, S.H.E. Kaufmann, J. Zerrahn, Modulation of T cell development and activation by novel members of the Schlafen (slfn) gene family harbouring an RNA helicase-like motif, Int. Immunol. 16 (2004) 1535–1548, https://doi.org/10.1093/intimm/dxh155.
- [51] E. Mavrommatis, E.N. Fish, L.C. Platanias, The Schlafen family of proteins and their regulation by interferons, J. Interf. Cytokine Res. 33 (2013) 206–210, https://doi. org/10.1089/jir.2012.0133.

[52] M. Mittal, M.R. Siddiqui, K. Tran, S.P. Reddy, A.B. Malik, Reactive oxygen species in inflammation and tissue injury, Antioxid. Redox Signal. 1 (20) (2014) 1126–1167, https://doi.org/10.1089/ars.2012.5149.

Data references

- [journal] [dataset] [6] G. Barturen, S. Babaei, F. Català-Moll, M. Martínez-Bueno, Z. Makowska, J. Martorell-Marugán, et al., Integrative analysis reveals a molecular stratification of systemic autoimmune diseases, Arthritis Rheumatol. 73 (2021) 1073–1085. ELIXIR, https://doi.org/10.17881/th
- [journal] [dataset] [7] Á. Fernández-Ochoa, C. Brunius, I. Borrás-Linares, R. Quirantes-Piné, M. de la L. Cádiz-Gurrea, null Precisesads Clinical Consortium, M.E. Alarcón Riquelme, A. Segura-Carretero, Metabolic Disturbances in Urinary and Plasma Samples from Seven Different Systemic Autoimune Diseases Detected by HPLC-ESI-QTOF-MS, J. Proteome Res. 19 (2020) 3220–3229. ELIXIR (2020), https://doi.org/10.17881/th9v-xt85.
- [other] [dataset] [9] B. Panwar, B.J. Schmiedel, S. Liang, B. White, E. Rodriguez, K. Kalunian, et al., Multi-cell type gene coexpression network analysis reveals coordinated interferon response and cross-cell type correlations in systemic lupus erythematosus, Genome Res. 31 (2021) 659-676., Gene Exp. Omnibus, (GEO) database (2021). GSE149050.